

Mechanism of Optically Inscribed High-Efficiency Diffraction Gratings in Azo Polymer Films

Christopher J. Barrett and Almeria L. Natansohn*

Department of Chemistry, Queen's University, Kingston, Ontario, Canada K7L 3N6

Paul L. Rochon

Department of Physics, Royal Military College, Kingston, Ontario, Canada K7K 5L0

Received: November 8, 1995; In Final Form: March 8, 1996[⊗]

A series of amorphous azobenzene-containing polymers were cast as thin films and shown to produce both reversible volume diffraction gratings and high-efficiency surface gratings by laser irradiation at an absorbing wavelength. The latter process involves localized mass transport of the polymer chains to a high degree, as atomic force microscopy reveals surface profile depths near that of the original film thickness. A mechanism for this phenomenon is proposed which involves pressure gradients as a driving force, present due to different photochemical behaviors of the azo chromophores at different regions of the interference pattern. The phase addition of the two beams in the interference pattern leads to regions of high trans-cis-trans isomerization by the absorbing azo groups, bordered by regions of low isomerization. As the geometrical isomerization requires free volume in excess of that available in the cast films, the photochemical reaction in these areas produces a laser-induced internal pressure above the yield point of the material. It is proposed that the resulting viscoelastic flow from these high-pressure areas to lower-pressure areas leads to the formation of the regularly spaced sinusoidal surface relief gratings observed by a number of research groups, but previously unexplained. This mechanism of photoinduced viscoelastic flow agrees well with the results of experiments investigating the effect of the polarization state of the interfering writing beams and the photochemical behavior of the chromophore, the free volume requirements of the induced geometric changes, and the viscoelastic flow of the material.

Introduction

There has been much recent interest in polymeric materials for holographic gratings in the fields of information storage, waveguide coupling, and nonlinear optoelectronics.^{1–4} Both volume refractive index and surface profile gratings can easily be formed, and polymer properties can be tailored to optimize the desired effect. Polymeric systems are commonly liquid crystalline,^{4,5–8} chromophore doped,^{9–11} or amorphous and covalently attached.^{1–3,12} The gratings in each case are produced with an interference pattern created from coherent laser light at a wavelength absorbed by the material. Depending on the polarization state of the incoming light, the interference is that of either intensity modulation¹³ or phase modulation,¹⁴ which can lead to either direct changes in absorption coefficient or refractive index¹⁵ or indirect optical changes involving molecular reorientation or mass transport.^{2,3,12} If a photoresist film is irradiated, subsequent wet chemistry has also been shown to produce a surface profile grating.¹⁶ While refractive index volume gratings are quickly written and can be erased, they display a relatively low efficiency due to the relatively small difference in refractive index that can be induced in the interference pattern. Much higher diffraction efficiencies are obtained with surface profile gratings, where large differences in path length can be employed. These systems with sinusoidal shape and depths greater than the probe wavelength approach the theoretical maximum for efficiency, achieved in volume gratings only with the rare class of nonlinear photorefractive systems.¹⁷

We have used amorphous high glass transition temperature (T_g) azo side chain polymers as materials for reversible optical

storage^{18,19} and have also reported their suitability for the writing of high-efficiency surface gratings.^{1,2} Tripathy³ and Kumar¹² have also produced high-efficiency surface gratings from azo side chain high- T_g polymers. They too observed large scale mass transport near room temperature and, like our previously published reports, confirmed that the azo isomerization is necessary and that grating formation is highly dependent on the polarization state of the laser beam. As both our group and theirs preclude ablation as a cause, this also concedes the role of bulk viscosity in the polymer films, as there must then be mass transport well below T_g . The diffraction gratings can be produced with a variety of polarization states of the writing laser and inscribed on polymers with a wide range of properties for study. These materials display various absorption maxima and coefficients, photochemical and isomerization behavior, and bulk viscosities of the films. The depth and spacing of inscribed surface profile gratings can be readily measured, and from examination of the role played by each of these parameters, a model is proposed here for the mechanism of surface grating formation in high- T_g azo polymer films. This mechanism involves the selective photoinduced isomerization of the azo groups and the free volume requirements of this geometrical transformation. The creation of free volume for the process where free volume is initially inadequate leads to pressure gradients above the yield point throughout the material, coincident with the light interference grating. The resulting viscoelastic flow in these low-viscosity polymers then leads to pressure-driven mass transport to form surface profile gratings suitable for high-efficiency diffraction. A brief review is presented, then, of the isomerization behavior of azo polymers, the resultant geometrical changes, and the associated bulk viscoelastic behavior.

[⊗] Abstract published in *Advance ACS Abstracts*, May 1, 1996.

The isomerization of the azo groups in these polymer films is key to the applications of photoinduced and eliminated birefringence, gratings, and switches.¹⁹ This readily induced and reversible geometric change is from the more stable *trans* isomer to the less stable *cis*.²⁰ With substitution of electron donor–electron acceptor groups in the para ring positions, the materials belong to the pseudostilbene spectral class,²¹ and both *trans* and *cis* isomers can be pumped with the same wavelength in the blue or green. In the absence of light there is a thermal relaxation from the *cis*-containing photostationary state to the *trans*-only state on the order of seconds,²² and the amount of *cis* present in these systems at the photostationary state can be measured indirectly by photochemical methods.^{23–25} Also key to all of our work is the selectivity of the $\pi \rightarrow \pi^*$ absorption of the *trans* dipoles to the polarization state of the irradiating light. The probability of absorption is proportional to $\cos^2 \phi$ where ϕ is the angle between the dipole axis and the electromagnetic field (EMF) vector of the laser light. Linearly polarized light will address only those dipoles lying with an orientational component parallel to the EMF vector, and circularly polarized light will address all dipoles except for those oriented along the light propagation axis. This selective isomerization and associated dipole reorientation have been well studied by our group as a mechanism for reversibly inducing dichroism and birefringence for optical storage.^{19,26}

The geometrical change associated with *trans*-to-*cis* isomerization of azobenzenes is significant and can be used to destroy or rearrange any ordered systems of *trans*-azobenzene groups such as in liquid crystalline phases,²⁷ ordered monolayer films,²⁸ or helical polymers.²⁹ The conversion from *trans*- to *cis*-azobenzene decreases the distance between the 4 and 4' ring positions from 10.0 to 5.6 Å³⁰ and increases the average free volume requirement to 0.2 nm³.³¹ Isomerization of azobenzenes has been well studied as a probe of free volume distribution in polymer matrices,^{32–34} as the kinetics of interconversion is sensitive to the local environment.

The viscoelastic behavior of azo polymer films is not as widely studied as the properties of isomerization and free volume morphology, but the phenomenon is general enough that order-of-magnitude calculations can be made from comparison with similar systems. The mechanical behavior of amorphous polymers below T_g can best be classified by examining the material's tensile strain (relative change in length in one dimension) that results from an applied stress (force per unit area).³⁵ Brittle polymers experience no flow of material under stress, and their resulting 1–2% elongation is due mainly to bending of bond angles and elongating bond lengths under high ($\sim 10^9$ Pa) stress at break.³⁶ Elastomeric polymers exhibit a similar stress/strain curve, though it is not linear, and achieve up to several hundred percent strain under only $\sim 10^4$ Pa stress.³⁵ In both cases if a brief stress before break is removed, the material returns reversibly to its initial state. An intermediate behavior on the stress/strain curve, and the behavior of interest here, is exhibited by tough plastics. These materials pass through a linear elastic region like that of elastomers or brittle plastics to a yield point, near $\sim 10^7$ Pa,³⁶ where the polymer chains begin to slide past each other and extensive elongation at constant stress ensues. Unlike the region of elasticity, this region of plastic flow is irreversible with the flow rate of the material governed by its bulk viscosity and driving force. Removal of the applied stress in this viscoelastic region produces an elastic return to equilibrium, with deformation and a new elastic region of the stress/strain curve. The resistance of the material to bulk deformation is the bulk modulus B , given by $B = P/\Delta V$ where P is the pressure and ΔV is the relative change in volume of the material.

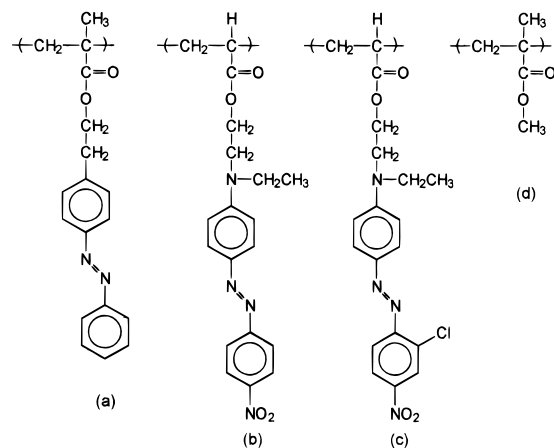


Figure 1. Structures of azo polymers studied. (a) PMEA, (b) PDR1A, (c) PDR13A, and (d) PMMA.

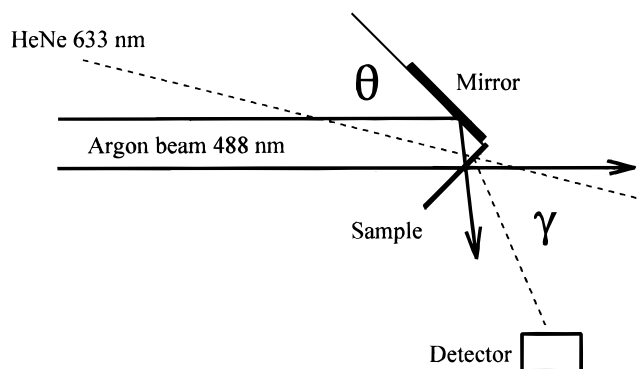


Figure 2. Experimental setup for grating inscription.

Experimental Section

The materials studied here are amorphous high- T_g polymers based on a substituted azobenzene side group and have been prepared, characterized, and reported previously.^{18,26,37–39} Their structures are detailed in Figure 1.

The polymers were dissolved in THF, spin-cast onto clean glass substrates, and heated to 95 °C to yield dry films of good optical quality and of thickness between 50 and 1200 nm. Molecular weights were determined by GPC relative to polystyrene, and film thickness determined by interferometry. T_g values were obtained by DSC, and densities of cast films were determined by pycnometry as previously reported.⁴⁰ *Cis* concentrations of irradiated films were determined by absorption spectra at the photostationary state similar to previous methods,^{23–25} and surface profiles of the gratings were recorded by a nanoscope II atomic force microscope (AFM). Poly(methyl methacrylate) (PMMA) blend samples were prepared by free radical polymerization of MMA in dry toluene at 60 °C for 24 h, using a range of AIBN initiator concentrations from 1% to 20% by mass. These polymers were purified by reprecipitation and blended with 50 wt % PDR1A to produce films of variable molecular weight.

The gratings were optically inscribed onto the films with a single beam split by a mirror and reflected coincident onto the film surface using the setup detailed in Figure 2. A 488 nm beam from an argon laser passed through a spatial filter and expanded to a diameter of 8 mm was used for writing.¹ The irradiation power ranged from 1 to 100 mW. Quarter wave plates were used to set the polarization state of the beam to linear (with the axis parallel to the mirror plane) or circular, and the progression of the grating inscription was monitored by measuring the growth of the first-order diffracted beam over

time with a 1 mW, 633 nm beam from a HeNe laser. Efficiencies were measured as the percentage of incident light intensity diffracted to a first-order beam at 633 nm, meeting the Bragg condition for thick gratings. Grating spacing was measured either by AFM or by measuring the angle of the diffracted beam. Microindentation studies were performed on 1 μm thick films indenting a diamond tip to a depth of 0.25 μm at a rate of 10 nm/s and recording the load.

Results

Irradiation of the polymer films as per the setup described in Figure 2 produces reversible volume birefringence gratings, reaching maximum efficiency in less than 2 s. AFM shows no resulting distortion of the film surface, and the efficiency of the grating, the ratio of the intensity of the first-order diffracted beam to the incident read beam intensity, is limited to about 0.3% for a 450 nm thick film of PDR1A, consistent with the level of birefringence known previously to be attainable with these films.¹ These volume gratings can be produced with the interference of either linearly or circularly polarized light beams, erased completely with brief exposure to a single linear or circular beam, and rewritten and erased repeatedly. The growth of this birefringence volume grating over time resembles the growth of induced birefringence in these films published previously²⁶ measured by the intensity of a 633 nm probe beam through crossed polarizers while the sample is illuminated with a linearly polarized beam of an absorbing wavelength. Another analogous feature of the birefringence volume grating inscription to the photoinduced birefringence is the independence of the magnitude of the effect on the irradiation intensity. With irradiation intensities varying from 5 to 200 mW/cm², the grating efficiencies at saturation are the same, though the rate of formation increases with laser power. In all cases the angle between the sample and the mirror is 90°, and the angle θ between the beam propagation axis and the mirror plane can be varied to produce the desired intensity profile spacing Λ_I . Λ_I can be calculated as

$$\Lambda_I = \lambda / (2 \sin \theta) \quad (1)$$

where λ is the wavelength of the writing beam. Gratings with Λ_I from 400 to 2000 nm have been produced. The volume grating diffracts a probe beam of wavelength λ' incident perpendicular to the film surface to an angle γ such that

$$\sin \gamma = \lambda' / \Lambda_b \quad (2)$$

where Λ_b is the period of birefringence in the grating. Measuring the diffracted angle γ for grating inscriptions of various θ values from 5° to 25° in increments of 2.5° shows that $\Lambda_b = \Lambda_I$ for all samples written with circularly or linearly polarized light. At $\theta > 23^\circ$ the grating spacing is exceeded by the wavelength of the probe beam and there is no solution to the diffracted beam (eq 2). Volume birefringence diffraction gratings can be written on all azobenzene polymers, copolymers, and polymer blends studied.

If the sample is exposed to the writing beam for longer than a few seconds, an irreversible process begins, creating an overlapping and highly efficient grating written on the time scale of minutes. Figure 3 displays the growth of the first-order diffracted beam for a sample of PDR1A so irradiated. There is an initial and rapid growth (on the order of seconds) of efficiency to about 1% corresponding to production of the reversible volume birefringence grating, and then a slower process (on the order of minutes) dominates up to high efficiency. The efficiency in these gratings ranges from 5% to

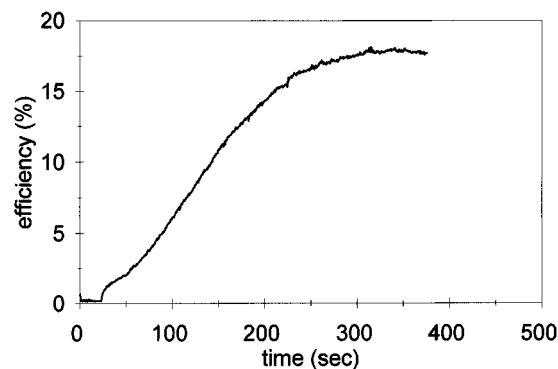


Figure 3. Growth of first-order diffraction over time in a PDR1A film.

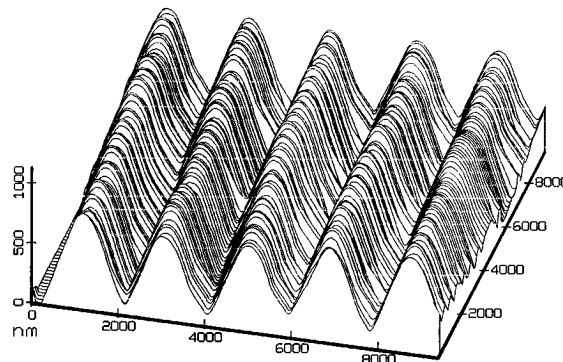


Figure 4. Atomic force microscope surface profile of an optically inscribed PDR13A grating.

45%, far beyond what can be achieved for solely a birefringent volume grating of these samples, and has been found to be due to a modulation of the surface of the film as AFM reveals a regularly spaced and sinusoidal surface relief grating coincident with the light intensity interference pattern. Depths from peak to trough of over 1000 nm have been achieved on samples whose initial film thickness was 1200 nm. A flattened profile in the troughs of some of the gratings suggests that the AFM tip had reached the glass substrate. Like the volume gratings, eq 2 is found to describe the diffraction of the probe beam and hence the period of the surface gratings. The surface profile period Λ_S is found to be equal to Λ_I and therefore matched Λ_b as well within experimental error. We had already established that the phase relationship between the surface and volume gratings coincides the light intensity maxima with the surface profile minima.² A typical grating profile for a PDR13A sample is presented in Figure 4. The efficiency is over 42% and the depth is near 900 nm. The efficiency of the gratings is proportional to grating depth, though this is difficult to quantify, as the efficiency depends also on the shape of the profile, reflection losses, and incidence angle of the probe beam. Once written, the grating profile is not photoerasable, remaining intact through irradiation with a single beam of either linearly or circularly polarized light or long-term exposure to moderate-power probe beams of either absorbing or nonabsorbing wavelengths. The gratings can be erased thermally, however, by heating the polymer film to T_g . Upon cooling the efficiency is reduced to zero, AFM shows an isotropic surface, and interferometry indicates no change in film thickness from the initial casting. The film can then be subsequently irradiated to produce a grating and then again erased and rewritten repeatedly. Once a grating is written, the writing geometry can be altered and another grating inscribed coincident with the first, either sharing the same fringe axis or rotated at an angle to the first. In this manner up to 10 coincident gratings have been stored, with good resolution of all first- and higher-order diffraction

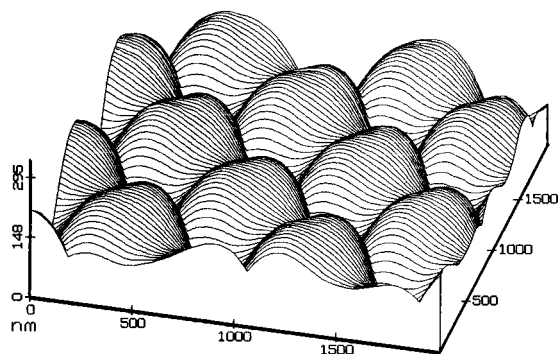


Figure 5. Atomic force microscope surface profile of two gratings inscribed consecutively after sample rotation of 90° .

spots for large spacing and also resolution of all argon laser fundamentals if so irradiated. As an example, Figure 5 displays the AFM surface profile of two such gratings written on a film of PDR1A rotated 90° between inscriptions. Like single gratings, multiple gratings are resistant to single linear or circular beams and can be erased only by heating to T_g . Even though the material has undergone substantial modification in surface profile, the azobenzene structural units can still be addressed in the same manner for inducing and erasing birefringence for reversible optical storage tests described previously.¹⁹ Photo-induced and eliminated birefringence can be performed in the gratings with similar rates, and achievable birefringence levels after losses due to diffraction had been taken into account. This suggests that the individual azo dipoles experience a similar environment before and after grating inscription, as the birefringence levels and writing rates are sensitive to local morphology and chromophore mobility.

The efficiency of the written gratings appears to depend on the nature of the irradiation, nature of the chromophores, and bulk properties of the polymer films. In order to investigate the role played in the grating inscription process by these three parameters, investigation concentrated on the effects of polarization, power, and geometry of the incident light, mobility and free volume requirements of the azo chromophores, and bulk viscosity of the polymer matrix.

Effect of the Writing Beams. Unlike the volume birefringence gratings, surface grating inscription shows a strong dependence on irradiation geometry, polarization of the writing beams, and laser power. The writing geometry can be varied by adjusting θ from 25° to 3° to give surface profile maxima spacings from 575 to 4600 nm. In agreement with the findings of Kumar,¹² diffraction efficiency displays a maximum at θ near 15° (spacing of 940 nm), decreasing at greater and lower irradiation angles. The efficiency is also observed to be strongly dependent on the polarization state of the writing laser. When linearly polarized light is used grating depths are limited to about 50 or 100 nm, while depths of 800–1100 nm can be inscribed using circularly polarized light on the same sample at the same power. Tripathy³ reports depths of 120 nm on similar materials using linearly polarized light. Figure 6 displays relative grating efficiency as a function of irradiation power for a sample of PDR13A. It is clear that both the writing rates and the maximum achievable efficiency are power dependent.

Effect of the Azo Chromophores. The mobility and free volume requirements of the chromophores strongly influence the extent of the grating inscription process. For surface gratings there are large differences in achievable efficiency between polymers with different azobenzene ring substituents. Similar to the findings of Tripathy and Kumar,¹² we have established that azo groups are necessary for the phenomenon, as irradiation of a film of an absorbing but nonisomerizing dye (rhodamine

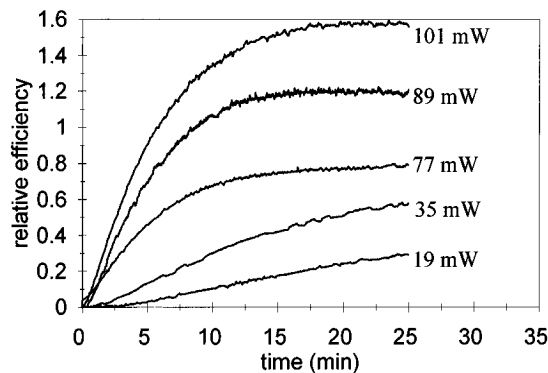


Figure 6. Relative diffraction efficiency of a PDR13A polymer film as a function of time at various irradiation intensities.

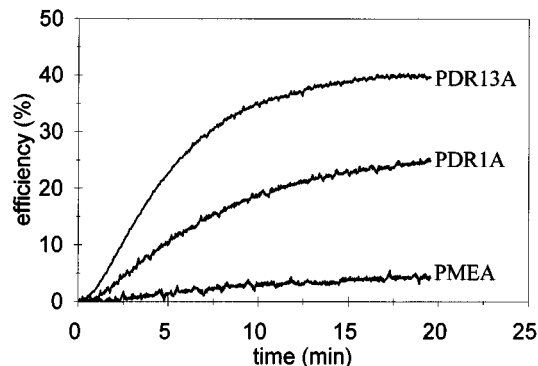


Figure 7. Diffraction efficiency vs time for polymers with various free volume requirements. PDR13A (upper trace), PDR1A (middle trace), and PMEAs (lower trace).

6G) produces no grating. Figure 7 illustrates the range of efficiencies achievable on films of different polymers. The films are of similar thickness, all near 800 nm, and irradiated at $\theta = 17.5^\circ$ with a 50 mW beam at 488 nm. The polymers PMEAs, PDR1A, and PDR13A are similar structurally,^{18,37} their main dissimilarity being the bulkiness of the azo group and hence the free volume required for isomerizing into the cis conformation. Although PMEAs does possess a lower extinction coefficient at the writing wavelength, this factor alone would not be sufficient to account for the substantial difference in the extent of grating formation observed between PMEAs and the polymers with bulkier azo chromophores. Estimates of the size and shape of the azo groups with these substituents can be made using molecular mechanics software and showed a van der Waals occupied volume of the isomerized azobenzene ring of 65 \AA^3 for PDR13A and 34 \AA^3 for PDR1A as compared to 23 \AA^3 for PMEAs. This suggests an increase in free volume required for the photoreaction of PDR13A (with the chloro- and nitro-substituted benzene ring) over PDR1A (with the nitrobenzene ring) over PMEAs with no ring substituents.

Effect of the Bulk Polymer Properties. The third set of the parameters investigated is the bulk properties of the polymer matrix. All copolymer samples of DR1A with MMA³⁸ produce gratings at moderate and high azo content similar to PDR1A, but compatible blends of PDR1A and PMMA³⁹ are not suitable for any surface grating formation, even at low PMMA content. The main difference between films of equal azo content copolymers and blends is the molecular weight and sequence distribution. The azo homopolymers and copolymers display molecular weights (MW) between 2000 and 10 000, to give an average degree of polymerization (DP) of around 10 structural units while the PMMA chains used for blending have MW > 300 000 (DP > 3000). In these samples only the volume birefringence gratings can be inscribed, and no modification of

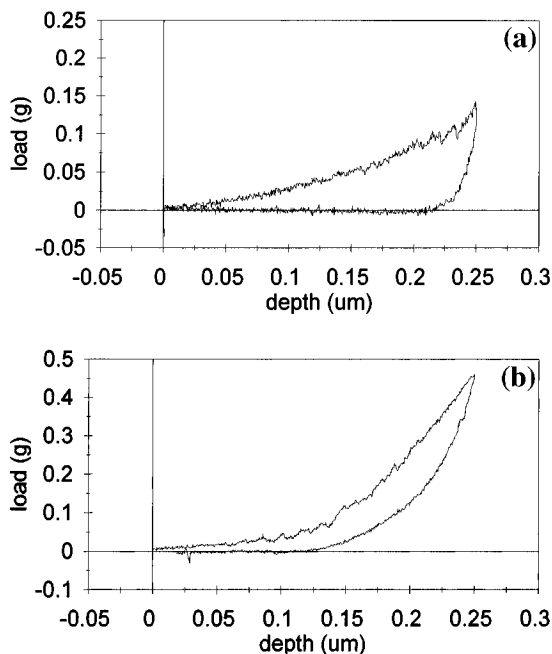


Figure 8. Load experienced on a diamond tip being microindented into the surface of a polymer film as a function of indentation depth. The upper trace follows the indentation of the tip and the lower trace its removal for (a) low-molecular weight 50% azo copolymer and (b) high-molecular weight 50% azo polymer blend.

the film surface can be induced. Microindentation studies on the low-MW copolymers and high-MW blends revealed that the molecular dissimilarity in chain length leads to a significant difference in bulk hardness of the cast films (Figure 8a,b). With a diamond tip indented 250 nm into the polymer films of thickness > 1000 nm, the load recorded at maximum depth for the high-MW blend is nearly 3 times that for the low-MW azo oligomer. In addition to the load experienced, there is a clear difference between the viscoelastic behavior of the two samples from the indentation and relaxation behavior (upper and lower traces respectively in Figure 8a,b). The return curve from deformation in the high-MW sample is similar to the indentation curve, suggesting elastic deformation, while in the low-MW sample the load drops sharply to zero on return, indicating a permanent deformation of the film surface. To study grating behavior intermediate to these two extremes, a MW series of short-chain PMMA hosts were prepared by free radical polymerization of MMA with various concentrations of initiator. This provided PMMA samples for blending with average molecular weights of 4000, 6300, 11 700, and 25 000 (DP = 40, 63, 117, and 250, respectively), in addition to commercially available PMMA with average molecular weights of 120K, 300K, and 1000K. PDR1A was blended into these hosts at 50 wt % and irradiated. Results are shown in Figure 9. A high-efficiency grating was inscribed on a film of the polymer blend with PMMA of lowest MW near that of the azo homopolymer, with a similar efficiency to PDR1A. With blends of higher-MW PMMA both the grating extent and inscription rate are diminished. With the blend of MW = 25 000 PMMA only the birefringence volume grating is produced (shown in Figure 9 lower trace), as it is for MW samples of 120 000, 300 000, and 1 000 000 MW PMMA. This volume-only grating behavior also shows the characteristic relaxation of the first-order signal after removal of the writing beams at $t = 80$ s, as well as complete erasure when irradiated with a single circular beam at $t = 150$ s. Grating production is then clearly dependent on the length of the polymer chains in the material undergoing mass transport.

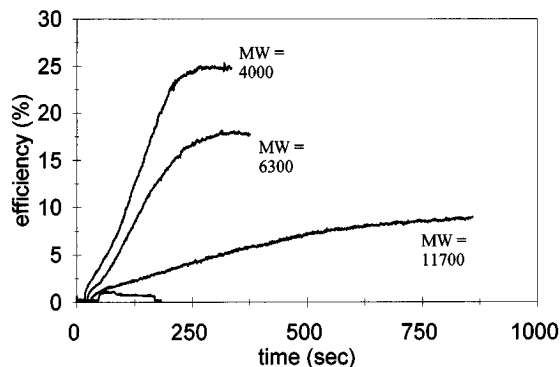


Figure 9. Growth of grating efficiency over time for PDR1A chromophores blended with various molecular weight PMMA polymers. The lower trace represents the volume grating-only behavior of all PMMA samples with MW > 25 000.

Discussion

By examining the nature of the light in the interference pattern and the resultant isomerization behavior of the azo groups, it becomes clear that pressure gradients produced in the interference pattern are large enough to provide a driving force for mass transport, dependent on the intensity of the light, free volume required for the photoisomerization, and viscosity of the polymeric material.

The two writing beams coincident on the sample are the reflected half and unreflected half of a single circularly polarized writing beam (Figure 2). At a region of interference, the net field is given by

$$E = 2E_0[\cos(kz - \omega t) \cos(\delta/2)]i + [-\cos(kz - \omega t) \sin(\delta/2) \cos \theta]j + [\sin(kz - \omega t) \cos(\delta/2) \sin \theta]k \quad (3)$$

where the components in each of the three orthogonal directions i , j , and k can be calculated as a function of θ and δ , the phase relationship (location in the repeating interference pattern from 0 to 2π). At phase delays of 0, $\pi/2$, and π , E is contained in the ik plane, j axis, and the ik plane again, respectively, creating a repeating pattern of elliptical, linear, elliptical, etc., polarizations with the ratio of components in each case dependent on θ .

In a mechanism similar to that previously reported as the basis of our reversible optical storage on azo films,⁴¹ dipoles absorbing polarized light will isomerize and randomly reorient into a position inert to the light polarization. This orientation will quickly saturate, inducing birefringence. Regions in the interference pattern containing two orthogonal EMF components (elliptical polarization) will address and isomerize all azo dipoles in the film plane, while the linear regions can only address dipoles lying on the polarization axis. This behavior is evident from the birefringent volume gratings, as the diffraction shows that there is a net saturation of orientation (low isomerization) in the regions of linear polarization and no birefringence (constant isomerization) in the regions of elliptical polarization. With a similar optical description, the coincidence of two beams whose polarization is linear creates an interference of intensity of linearly polarized light in the sample, resulting in linear regions which orient the dipoles and regions of no isomerization retaining the film isotropy. With irradiation of either circularly polarized light (alternating regions of unselective and selective isomerization) or linearly polarized light (alternating regions of selective and no isomerization), the end result is the same. Brief irradiation produces regularly spaced regions of oriented and unoriented azo groups, leading to the periodic birefringence

observed as a grating. With the writing of surface profile gratings, however, this difference in isomerization behavior becomes significant. As the mass transport necessary to create deep crests and troughs appears to be driven by isomerization pressure, the orientation of the dipoles becomes less significant than their rate of isomerization. The interference of two circularly polarized beams creates alternating regions of high (elliptical) and low (linear) isomerization, while the interference of two linearly polarized beams creates alternating regions of low (linear) and no (completely destructive interference) isomerization. The effect of a pressure gradient between the regions is similar, but greatly diminished in the latter case. It is also apparent from eq 3 that the constructed elliptical polarization will be most circular (address the largest number of dipole orientations and lead to the largest pressure gradient) at an intermediate value of θ . This is supported experimentally by the dependence of grating efficiency on θ , showing a maximum near $\theta = 15^\circ$. With this pressure gradient as the driving force, the extent of the phototransport would be expected to depend on the irradiation power as well, in agreement with observations. For a sample of low-MW azo polymer irradiated with writing beams of circular polarization, order of magnitude estimates can be made of the magnitude of this photoinduced pressure and the associated response of the viscoelastic material.

Considering the case of PDR1A, it has already been shown using previously published photochemical methods²⁴ that cis concentrations in the photostationary state range from 5% to 10%, depending on laser power and temperature, and that initially the film contains virtually all azo groups in the trans conformation.⁴² With a film density of 1.3 g/cm^3 ⁴⁰ and estimated van der Waals occupied volume in the film of 67%,³¹ an arbitrary volume of 1 cm^3 of azo polymer film contains 0.67 cm^3 of polymer and 0.33 cm^3 average free volume per chromophore. Isomerization to the cis geometry and the dissipation of the large amount of thermal energy of the cis isomer require 0.77 cm^3 average free volume as a conservative estimate for an azobenzene unsubstituted by bulky groups.³¹ These numbers are average cavity sizes, but the distribution of free volume in PMMA has been shown to be relatively narrow.³¹ With a constant energy flux isomerizing up to a 5% cis photostationary region in the regions of high isomerization, this represents a required volume increase of 0.8% in these regions. The pressure exerted by this volume change can be estimated with B , the bulk modulus of the material which relates P to ΔV as $P = B(\Delta V/V)$. Using a figure of $B = 3 \times 10^9 \text{ Pa}$,³⁶ the pressure can now be estimated as $2.5 \times 10^7 \text{ Pa}$, comparable to the estimated yield point for these polymers of $2 \times 10^7 \text{ Pa}$.³⁶ This isomerization pressure represents a driving force, as the dynamic equilibrium will hold the cis fraction (and hence pressure) constant under irradiation. With stress above the yield point in the polymer in these regions viscoelastic flow results, with a rate dependent on the polymer bulk viscosity and an extent depending indirectly on the viscosity as well. As material is removed from the regions of high isomerization and builds up in the regions of low isomerization, there appears to be an opposing or restoring force, perhaps due to the surface tension. In the case of linearly polarized writing beams with alternating regions of low and no isomerization, the driving force is diminished, as the pressure gradient between low and no isomerization regions of a linear interference pattern is less than that between regions of high and low isomerization of the interference between circular beams. This would serve to lessen the extent of phototransport, as observed.

Also in agreement with our observations, a greater free

volume requirement of the chromophore would result in a higher-pressure driving force. With polymers of similar T_g and molecular weight, the chromophores with the largest free volume requirement produced the deepest and highest-efficiency gratings. With these bulky chromophores an increase in driving force would be expected, equaled by the opposing force only after substantial surface modification.

As the viscosity is dependent on the size of the chains, in polymers of higher molecular weight the rate and extent of grating formation should also be decreased, as observed. In polymers with high enough molecular weight (i.e., the high-MW PMMA blends), there should be no expected mass transport at all, as the yield point will be higher on the stress/strain curve, inaccessible under the conditions studied. The bulk viscosity of polymers is generally observed to increase with the first power of the molecular weight ($\eta \propto \text{MW}$) up to the limit of entanglement and then increases rapidly with MW to the power of at least the cube ($\eta \propto \text{MW}^{3.4}$) after this point.³⁶ From studies of polymers in melt flow, this entanglement limit has been reported to be near 40 000 for PMMA.³⁶ Incorporation of chains as long or longer than this into the system appears to prohibit phototransport and grating formation completely and effectively, as blending even 5% long-chain PMMA into PDR1A renders the films inert to the inscription process. In this case the yield point is greater than the photoinduced pressure achievable in the gratings, and although the isomerization produces the same pressure, the process is limited to the elastic region of the stress strain curve and the surface is prevented from deforming. The results from the variable-MW series of PMMA blended with PDR1A show that when molecular weights are increased above those of the azo homopolymers (but below the limit of entanglement), there is a decrease in both the inscription rate and grating depth achievable, up to a point where phototransport is prevented by the high viscosity of the entangled bulk polymer. This limit appears to be reached between samples of $\text{MW} = 11\,700$ and $25\,000$, a lower molecular weight than the reported entanglement limit for PMMA, though this limit would be expected to be lowered substantially in the systems studied here with large chromophore side chains. The process is most likely aided as well by localized temperature increases from the highly absorbing azo groups. This would serve to lower the bulk viscosity and increase the rate of grating formation. There had been some early speculation that the grating formation may be temperature driven,^{2,3} but although temperature probably plays some role, the increase in temperature in isomerized regions has been estimated to be a relatively small 5°C .⁴⁴ The fact that irradiation of film of an absorbing yet nonisomerizing polymer system (dispersed rhodamine 6G) produced no detectable surface features confirms that temperature is not a dominant factor. Recent publications suggesting a depression of the T_g near the surface of thin films^{45,46} would also enhance the mass transport, though effects were reported to be minimal below 30 or 40 nm from the film surface.

Conclusions

Both volume refractive index and surface profile diffraction gratings could be laser inscribed in azo polymer thin films. The mechanism for the high-efficiency photoinduced surface gratings appears to be isomerization driven mass transport, with grating depths of up to $1 \mu\text{m}$ achievable with films of an initially similar thickness. This proposed phototransport mechanism agrees well with results of studies varying the nature of the writing laser, free volume requirements of the chromophores, and bulk viscosity of the polymer matrix.

Acknowledgment. Funding was provided by the Office of Naval Research USA, NSERC Canada, and the Department of National Defence Canada. The authors thank Scott Noel of the Department of Physics, R.M.C. for AFM testing, and William Newson of the Department of Materials Science Engineering, Queen's University, for microindentation testing. A.N. is grateful to the Canada Council for a Killam Research Fellowship.

References and Notes

- (1) Rochon, P.; Mao, J.; Natansohn, A.; Batalla, E. *Polym. Prepr. (Am. Chem. Soc., Polym. Chem.)* **1994**, *35* (2), 154.
- (2) Rochon, P.; Batalla, E.; Natansohn, A. *Appl. Phys. Lett.* **1995**, *66*, 136.
- (3) Kim, D. Y.; Tripathy, S. K. *Appl. Phys. Lett.* **1995**, *66*, 1166.
- (4) Bieringer, T.; Wuttke, R.; Haarer, D.; Gessner, U.; Rübner, J. *Macromol. Chem. Phys.* **1995**, *196*, 1375.
- (5) Hvilsted S.; Andruzzi, F.; Kulinna, C.; Siesler, H.; Ramanujam, P. *Macromolecules* **1995**, *28*, 2172.
- (6) Chen, A. G.; Brady, D. J. *Opt. Lett.* **1992**, *17*, 441.
- (7) Wuttke, R.; Fischer, K.; Bieringer, T.; Haarer, D.; Eisenbach, C. D. *Polym. Mater. Sci. Eng.* **1995**, *72*, 520.
- (8) Eich, M.; Wendorff, J. H.; Reck, B.; Ringsdorf, H. *Macromol. Chem. Rapid Commun.* **1987**, *8*, 59.
- (9) Fei, H.; Wei, Z.; Wu, P.; Han, L.; Zhao, Y.; Che, Y. *Opt. Lett.* **1994**, *19*, 411.
- (10) Xu, J.; Zhang, G.; Wu, Q.; Liang, Y.; Liu, S.; Sun, Q.; Chen, X.; Shen, Y. *Opt. Lett.* **1995**, *20*, 504.
- (11) Wang, C. H.; Xia, J. L. *J. Phys. Chem.* **1992**, *96*, 190.
- (12) Kim, D.; Li, L.; Jiang, X.; Shivshankar, V.; Kumar, J.; Tripathy, S. *Macromolecules* **1995**, *28*, 8835.
- (13) Eich, M.; Wendorff, J. H. *Macromol. Chem. Rapid Commun.* **1987**, *8*, 467.
- (14) Ortler, R.; Bräuchle, C.; Miller, A.; Riepl, G. *Makromol. Chem. Rapid Commun.* **1989**, *10*, 189.
- (15) Todorov, T.; Nikolova, L.; Tomova, N. *Appl. Opt.* **1984**, *23*, 309.
- (16) Johnson, L.; Kammlott, G.; Ingersoll, K. *Appl. Opt.* **1978**, *17*, 1165.
- (17) Meerholz, K.; Volodin, B. L.; Sandalphon, K.; Kippelen, B.; Peyghambarian, N. *Nature* **1994**, *371*, 497.
- (18) Natansohn, A.; Rochon, P.; Gosselin, J.; Xie, S. *Macromolecules* **1992**, *25*, 2268.
- (19) Xie, S.; Natansohn, A.; Rochon, P. *Chem. Mater.* **1993**, *5*, 403.
- (20) Kumar, G.; Neckers, D. *Chem. Rev.* **1989**, *89*, 1915.
- (21) Rau, H. In *Photochemistry and Photophysics*; Rabek, J. F., Ed.; CRC Press: Boca Raton, FL, 1990; Vol. 2, Chapter 4.
- (22) Barrett, C.; Natansohn, A.; Rochon, P. *Chem. Mater.* **1995**, *7*, 899.
- (23) Fischer, E. *J. Phys. Chem.* **1967**, *71*, 3704.
- (24) Rau, H.; Greiner, G.; Gauglitz, G.; Meier, H. *J. Phys. Chem.* **1990**, *94*, 6523.
- (25) Biswas, N.; Umopathy, S. *Chem. Phys. Lett.* **1995**, *236*, 24.
- (26) Natansohn, A.; Xie, S.; Rochon, P. *Macromolecules* **1992**, *25*, 5531.
- (27) Anderle, K.; Birenheide, R.; Eich, M.; Wendorff, J. H. *Makromol. Chem. Rapid Commun.* **1989**, *10*, 477.
- (28) Seki, T.; Tamaki, T. *Chem. Lett.* **1993**, 1739.
- (29) Müller, M.; Zentel, R. *Macromolecules* **1994**, *27*, 4404.
- (30) Sato, M.; Kinoshita, T.; Takizawa, A.; Tsujita, Y. *Macromolecules* **1988**, *1*, 1612.
- (31) Naito, T.; Horie, K.; Mita, I. *Polymer* **1993**, *34*, 4140.
- (32) Eisenbach, C. D. *Makromol. Chem.* **1978**, *179*, 2489.
- (33) Sasaki, T.; Ikeda, T.; Ichimura, K. *Macromolecules* **1993**, *26*, 151.
- (34) Kim, Y.; Paik Sung, C. S.; Kim, Y. *Macromolecules* **1995**, *28*, 6198.
- (35) Ferry, J. D. *Viscoelastic Properties of Polymers*, 3rd ed.; John Wiley: New York, 1980; Chapter 1.
- (36) Sperling, L. H. *Physical Polymer Science*, John Wiley: New York, 1986; Chapter 6.
- (37) Natansohn, A.; Rochon, P.; Ho, M.; Barrett, C. *Macromolecules* **1995**, *28*, 4179.
- (38) Xie, S.; Natansohn, A.; Rochon, P. *Macromolecules* **1994**, *27*, 1489.
- (39) Xie, S.; Natansohn, A.; Rochon, P. *Macromolecules* **1994**, *27*, 1885.
- (40) Brown, D.; Natansohn, A.; Rochon, P. *Macromolecules* **1995**, *28*, 6116.
- (41) Rochon, P.; Gosselin, J.; Natansohn, A.; Xie, S. *Appl. Phys. Lett.* **1992**, *60*, 4.
- (42) Barrett, C. M.Sc. Thesis, Queen's University, 1994.
- (43) Lopez, J. *Polym. Test.* **1993**, *12*, 437.
- (44) Bauer-Gogonea, S.; Bauer, S.; Wirges, W.; Gerhard-Multhaupt, R. *J. Appl. Phys.* **1994**, *76*, 2627.
- (45) Keddie, J.; Jones, R.; Cory, R. *Europhys. Lett.* **1994**, *27*, 59.
- (46) Keddie, J.; Jones, R.; Cory, R. *Faraday Discuss.* **1994**, *98*, 219.